Uncovering the mystery of X(3872) with the coupled channel dynamics

Jun-Zhang Wang (王俊璋)

重庆大学& 北京大学

Based on arXiv: 2404.16575
Together with 林子阳, 陈炎柯, 孟璐和朱世琳教授

2025.04.14 湖南师范大学@长沙

Outline

- The pole origin of X(3872) with the coupled channel dynamics
- A novel approach to reveal the nature of X(3872)
- Summary

$D\bar{D}^*$ (1^{++}) X(3872)

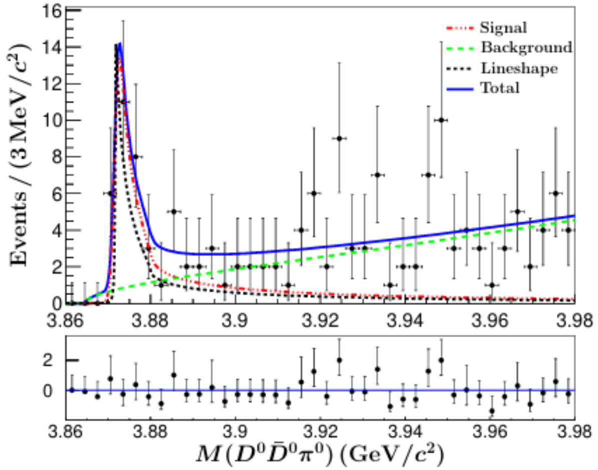

Phys. Rev. Lett. 91 (2003) 262001

Phys. Rev. Lett. 132 (2024) 15, 151903

$D\bar{D}^*$ (1^{+-}) Zc(3900)

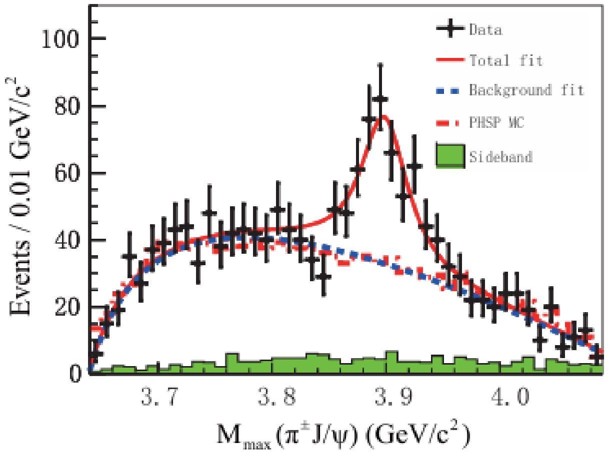

Phys. Rev. Lett. 110 (2013) 252001

DD^* (1^{+}) Tcc

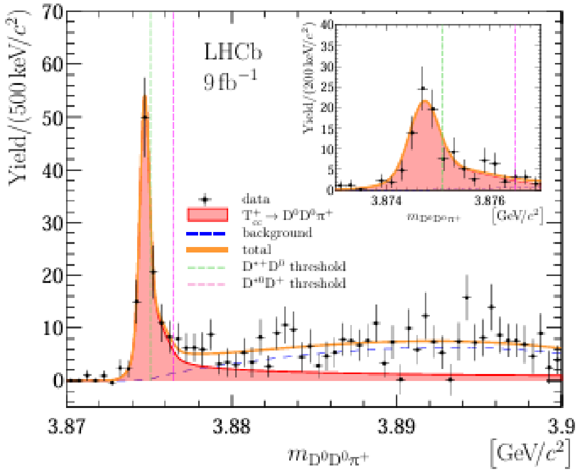

Nature Commun. 13 (2022) 3351

$D\bar{D}^*$ (1^{--}) G(3900)

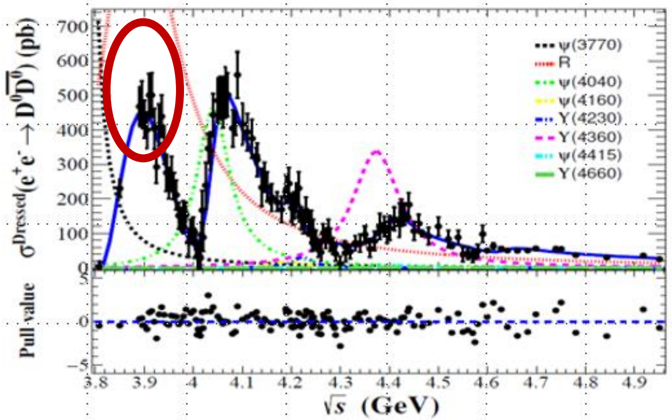

Phys. Rev. Lett. 133 (2024) 8, 081901

Hadronic molecular explanation

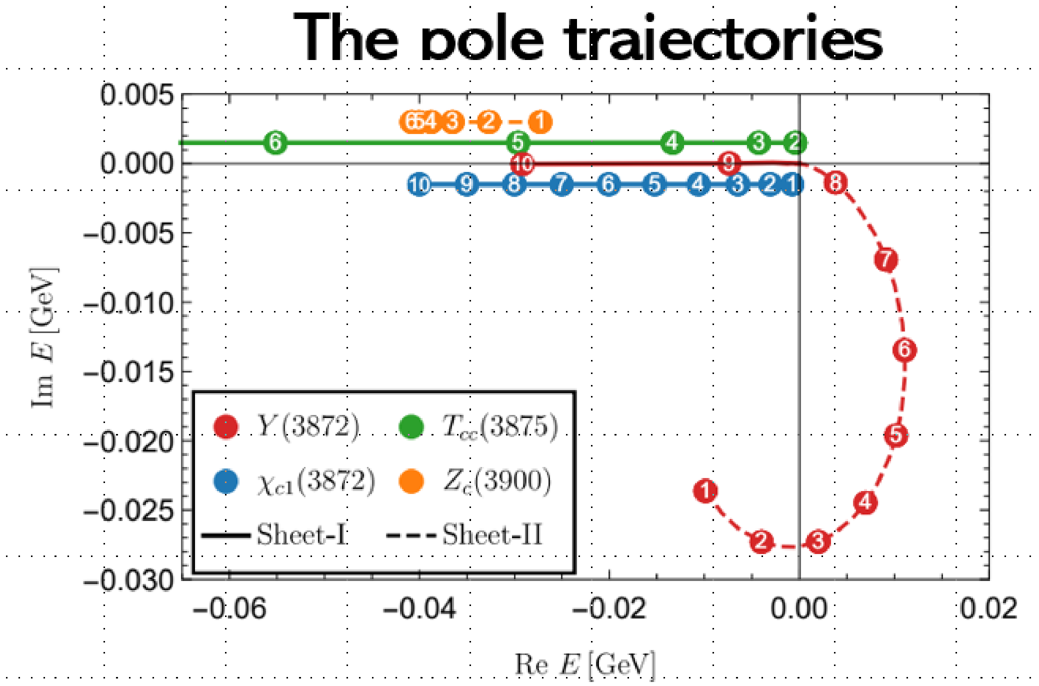

Z.Y. Lin, J.Z. Wang, J.B. Cheng, L. Meng and S.L. Zhu,

Phys. Rev. Lett. 133 (2024) 24, 241903

The unquenched quark model

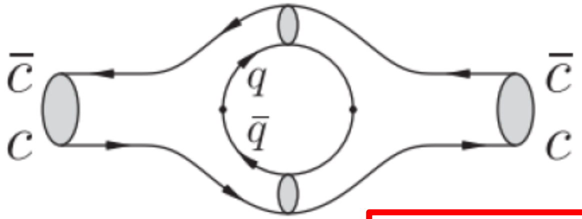

$$m_{\rm phy}^2 = m_{\rm bare}^2 + {\rm Re}\Pi(m_{\rm phy}^2), \quad \Gamma = -\frac{{\rm Im}\Pi(m_{\rm phy}^2)}{m_{\rm phy}}$$

Multiplet	State ($n^{2S+1}L_J$)	J^{PC}	PDG State	Expt. mass	Expt. width	Re[$\sqrt{s_{pole}}$]	Im[$\sqrt{s_{pole}}$]	GI mass
3S	$\psi(3^3S_1)$	1^{--}	$\psi(4040)$	4039±1	80±10	4051	25	4100
	$\eta_c(3^1S_0)$	0^{-+}				4025	23	4064
4S	$\psi(4^3S_1)$	1^{--}	$X(4360)$	4361±13	74±18	4371	49	4450
	$\eta_c(4^1S_0)$	0^{-+}				4348	48	4425
2P	$\chi_2(2^3P_2)$	2^{++}	χ'_{c2}	3927±2	24±6	3942	2	3979
	$\chi_1(2^3P_1)$	1^{++}	$X(3872)$	3872	<2.3	3884	4	3953
	$\chi_0(2^3P_0)$	0^{++}	$X(3880)$?	3878±48?	347^{+316}_{-143}?	3814	133	3916
	$h_c(2^1P_1)$	1^{+-}	$X(3940)$	3942±9	37^{+27}_{-17}	3900	6	3956
3P	$\chi_2(3^3P_2)$	2^{++}				4244	24	4337
	$\chi_1(3^3P_1)$	1^{++}				4217	84	4317
	$\chi_0(3^3P_0)$	0^{++}	$X(4160)$	4160^{+29}_{-25}	139^{+110}_{-60}	4210	114	4292
	$h_c(3^1P_1)$	1^{+-}				4219	49	4318
1D	$\psi_3(1^3D_3)$	3^{--}				3838	1	3849
	$\psi_2(1^3D_2)$	2^{--}						3838
	$\psi(1^3D_1)$	1^{--}	$\psi(3770)$	3773	27±1	3764	18	3819
	$\eta_{c2}(1^1D_2)$	2^{-+}						3837
2D	$\psi_3(2^3D_3)$	3^{--}				4113	6	4217
	$\psi_2(2^3D_2)$	2^{--}				4141	72	4208
	$\psi(2^3D_1)$	1^{--}	$\psi(4160)$	4153±3	103±8	4080	114	4194
	$\eta_{c2}(2^1D_2)$	2^{-+}				4101	44	4208

Eur. Phys. J. A 50, no.10, 165 (2014)

P-wave charmonium explanation

M. R. Pennington and D. J. Wilson, Decay channels and charmonium mass-shifts, Phys. Rev. D **76**, 077502 (2007), arXiv:0704.3384 [hep-ph].

S. Ono and N. A. Tornqvist, Continuum Mixing and Coupled Channel Effects in $c\bar{c}$ and $b\bar{b}$ Quarkonium, Z. Phys. C **23**, 59 (1984).

B.-Q. Li, C. Meng, and K.-T. Chao, Coupled-Channel and Screening Effects in Charmonium Spectrum, Phys. Rev. D **80**, 014012 (2009), arXiv:0904.4068 [hep-ph].

⋮

Recent works from different groups based on the charmonium assumption of X(3872)

Phys.Rev.D 108 (2023) 9, 094046 (Production)

Phys.Lett.B 848 (2024) 138404 (decay)

Phys.Rev.D 111 (2025) 5, 054021 (Production)

The coupled-channel dynamics

The general coupled-channel equation

$$|\Phi\rangle = c_0|\Phi_0\rangle + \sum_i \int \frac{d^3\mathbf{q}}{(2\pi)^3}\phi_i(\mathbf{q})|\Phi_i\rangle_{\mathbf{q}},$$

$$\begin{pmatrix} \mathcal{H}_0 & \mathcal{H}_{01} & \mathcal{H}_{02} & \dots \\ \mathcal{H}_{10} & \mathcal{H}_1 & \mathcal{H}_{12} & \dots \\ \mathcal{H}_{20} & \mathcal{H}_{21} & \mathcal{H}_2 & \dots \\ \vdots & \vdots & \vdots & \ddots \end{pmatrix} \begin{pmatrix} c_0|\Phi_0\rangle \\ |\Phi_1\rangle \\ |\Phi_2\rangle \\ \vdots \end{pmatrix} = E \begin{pmatrix} c_0|\Phi_0\rangle \\ |\Phi_1\rangle \\ |\Phi_2\rangle \\ \vdots \end{pmatrix}$$

$$\sum_i (\delta_{ij}E_k + \int (V_{ij}(\mathbf{q},\mathbf{q}') + \mathcal{V}_{ij}(\mathbf{q},\mathbf{q}'))\phi_i(\mathbf{q}')\frac{d^3\mathbf{q}'}{(2\pi)^3}) = E\phi_j(\mathbf{q}) \quad (j = 1,2,3\dots), \qquad (6)$$

$$\mathcal{V}_{ij}(\mathbf{q},\mathbf{q}') = \frac{\mathcal{V}_{i0}(\mathbf{q}')\mathcal{V}_{0j}(\mathbf{q})}{E - M_0 + i\epsilon}$$

The coupled-channel problem involving the bare pole and continuum states can be converted to be a hadron-hadron scattering problem

The chiral effective field theory (ChEFT)

$D\bar{D}^* \to D\bar{D}^*$

$$|C = \pm\rangle = \frac{1}{\sqrt{2}}(|D(\mathbf{p})\bar{D}^*(-\mathbf{p})\rangle \mp |\bar{D}(\mathbf{p})D^*(-\mathbf{p})\rangle)$$

$$V_{\text{Total}}(\mathbf{q},\mathbf{q}') = \begin{pmatrix} C_t - V_{\pi^0} + \mathcal{V}_{11} & C_t' - 2V_{\pi^\pm} + \mathcal{V}_{12} \\ C_t' - 2V_{\pi^\pm} + \mathcal{V}_{21} & C_t - V_{\pi^0} + \mathcal{V}_{22} \end{pmatrix}$$

The coupled-channel Lippmann-Schwinger equation (LSE)

$$T^\alpha_\beta(q,q') = V^\alpha_\beta(q,q') + \sum_\gamma \int_0^\infty \frac{dkk^2}{(2\pi)^3}\frac{V^\alpha_\gamma(q,k)T^\gamma_\beta(k,q')}{E - k^2/(2\mu_\gamma)}$$

$$\mu_\gamma = \frac{m_1 m_2}{m_1 + m_2}.$$

The regulator : $\mathcal{F}(\mathbf{q},\mathbf{q}') = \exp(-(\mathbf{q}^2 + \mathbf{q}'^2)/\Lambda^2).$

The pole origin of X(3872) in the single channel case

The S-wave s-channel potential

$$\mathcal{V} = \frac{g^2}{2M_0} e^{-(\mathbf{q}^2+\mathbf{q}'^2)/\alpha^2} / (E - M_0 + i\epsilon)$$

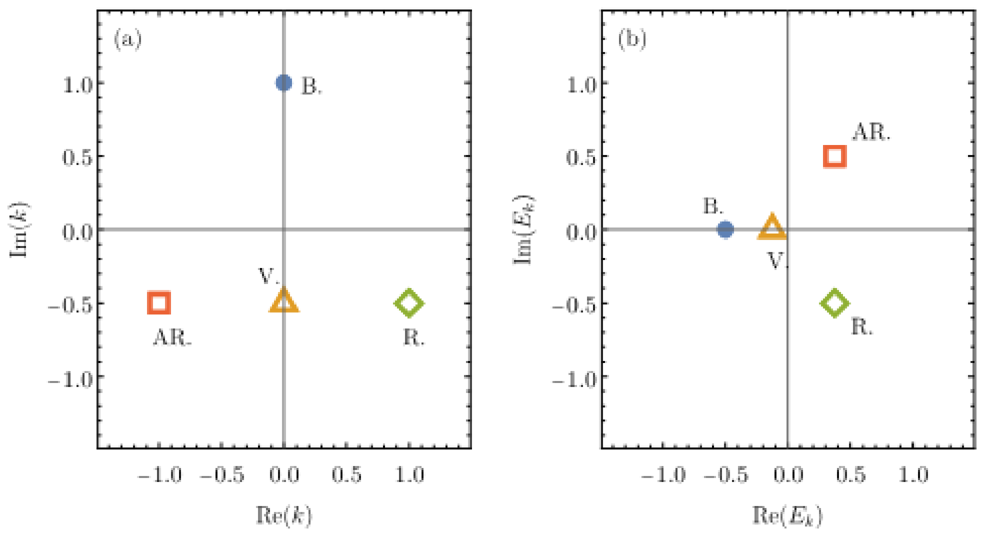

bound states:	$k_B = i\gamma_b$	(RS-I),
virtual states:	$k_V = -i\gamma_v$	(RS-II),
resonances:	$k_R = \kappa_r - i\gamma_r$	(RS-II),
antiresonances:	$k_{AR} = -\kappa_r - i\gamma_r$	(RS-II).

The weak coupling mode

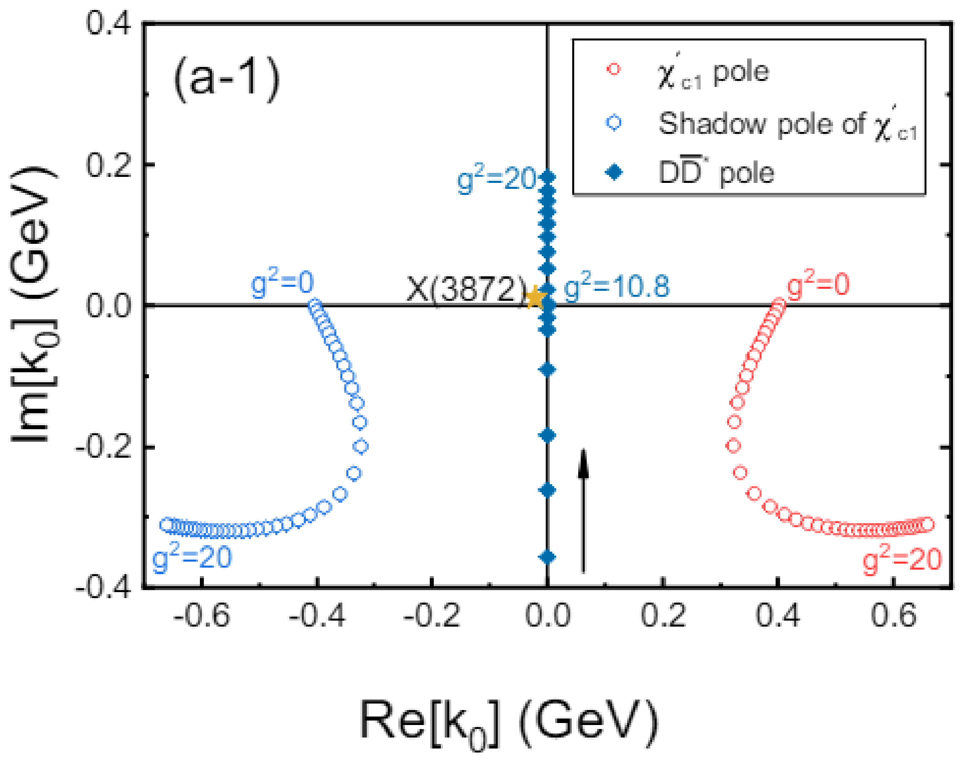

The same phenomenon with the two-pole structure in the talk of prof. Zhi-Yong Zhou

The strong coupling mode

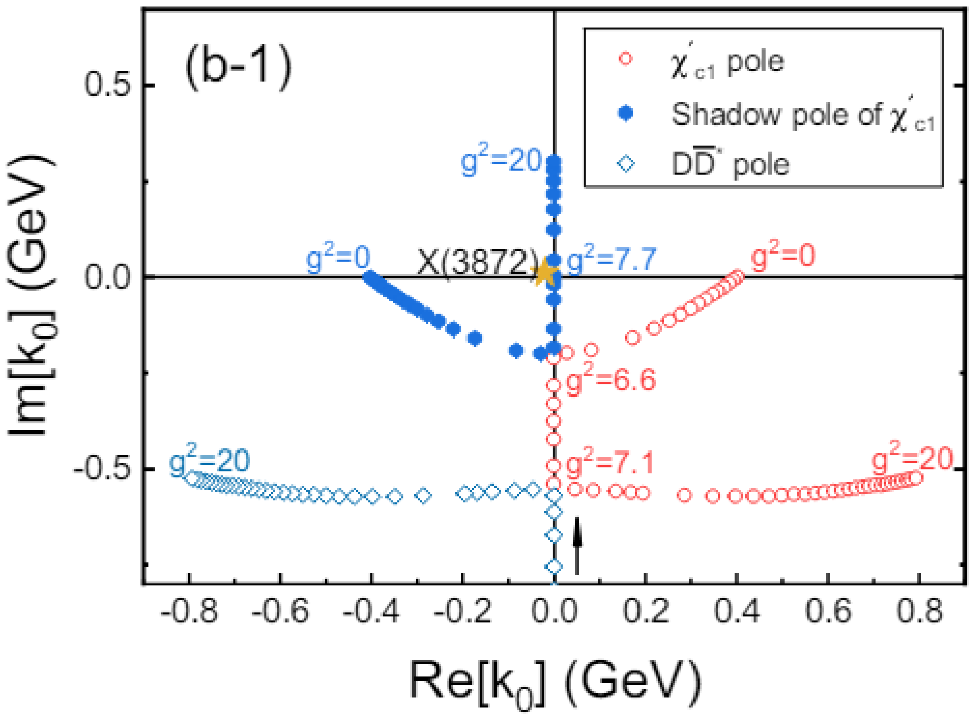

The inclusion of the contact interaction of $D\bar{D}^*$

Attractive force

Repulsive force

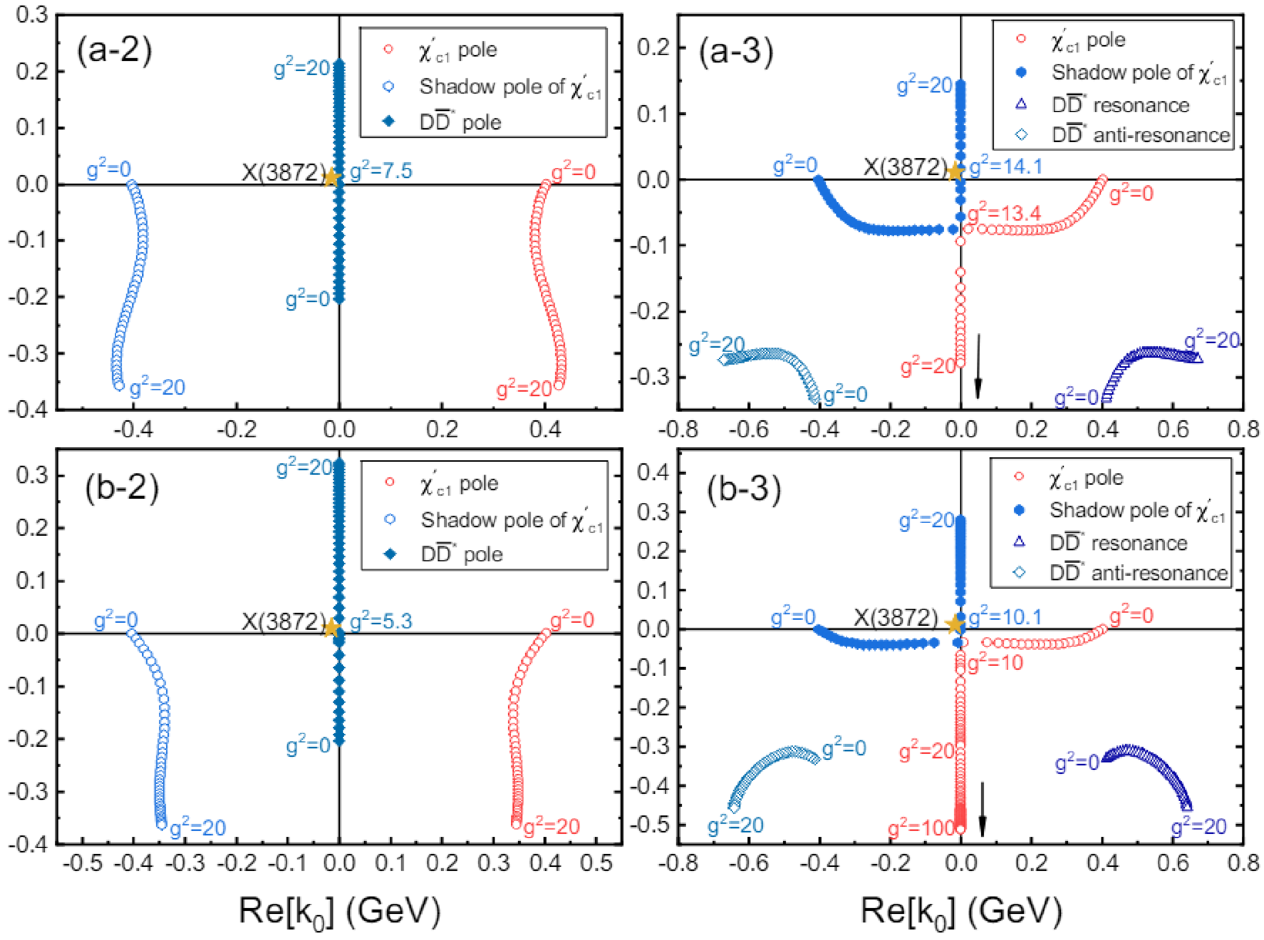

The pole origin of X(3872) in the coupled channel case

Uniformization

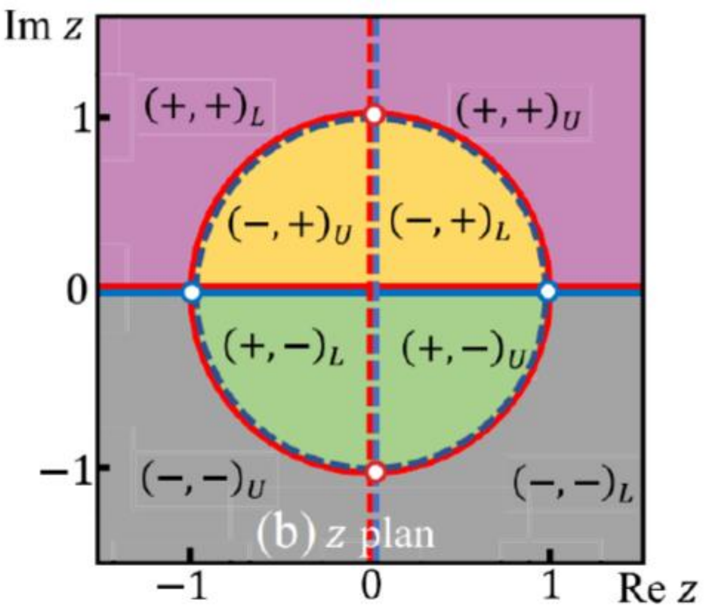

$$p_0^2 = E^2 - m_{th0}^2, \quad p_\pm^2 = E^2 - m_{th\pm}^2,$$

$$p_\pm + p_0 = \Delta z, \quad p_0 - p_\pm = \frac{\Delta}{z}.$$

Phys. Rev. D 107 (2023) 1, 014005

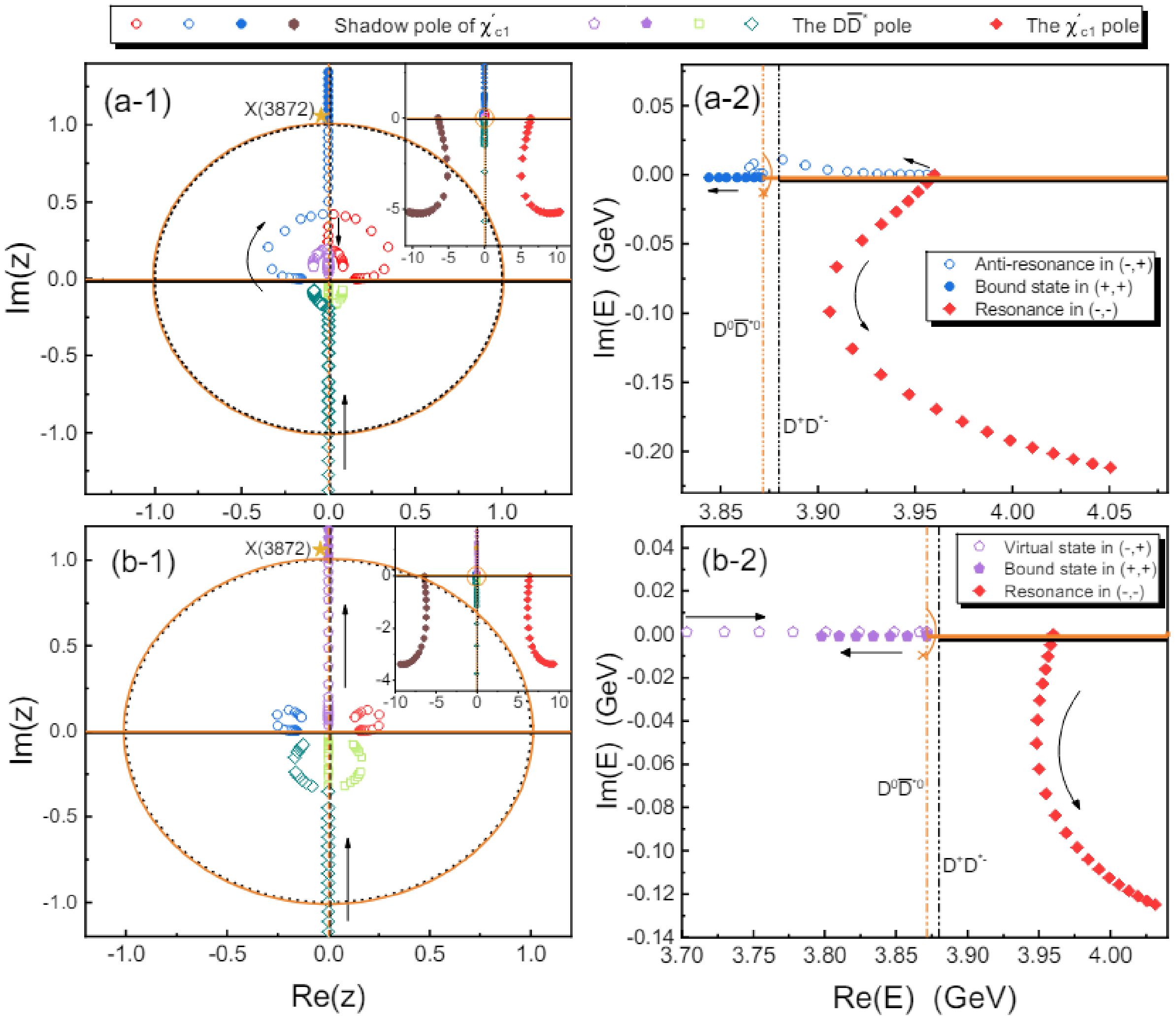

Our definite conclusion: X(3872) does not stem from the mass shift of the bare charmonium $\chi_{c1}(2P)$ state!

The complete analysis and pole width of X(3872)

$$\delta m_{\rm pole} = -360 \pm 40\ \mathrm{keV},\quad \Gamma_{\rm pole} = 48 \pm 2\ \mathrm{keV}$$

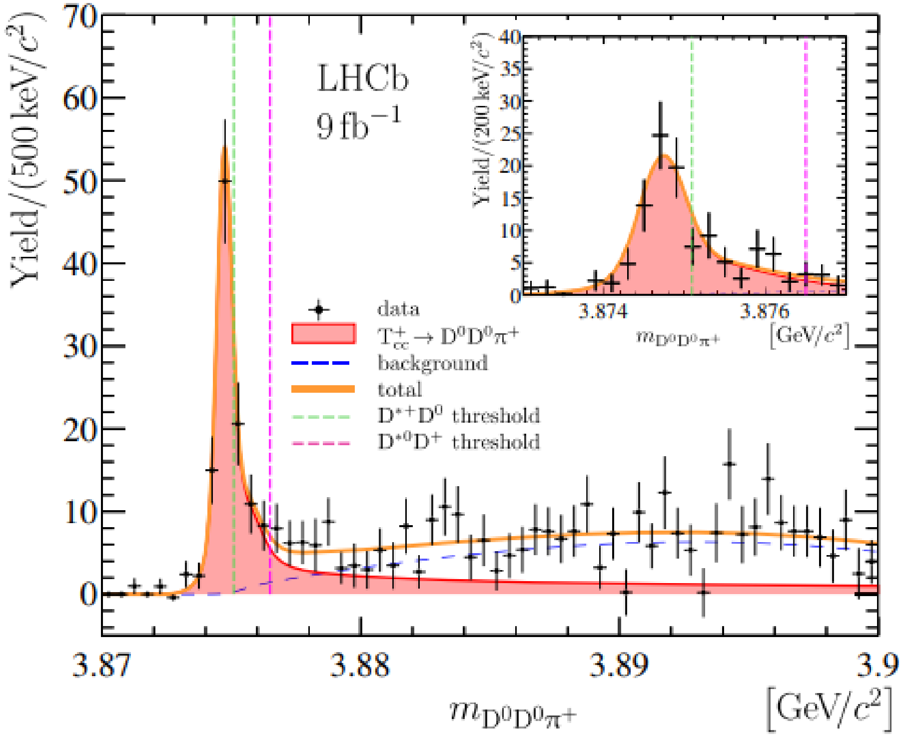

Nature Commun. 13, no.1, 3351 (2022)

Three-body threshold cut

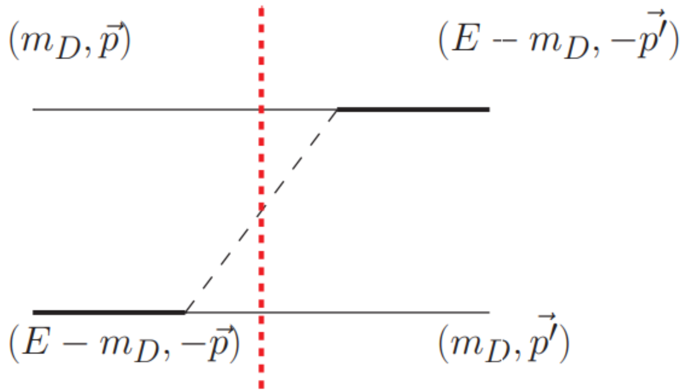

Self-energy of D^*

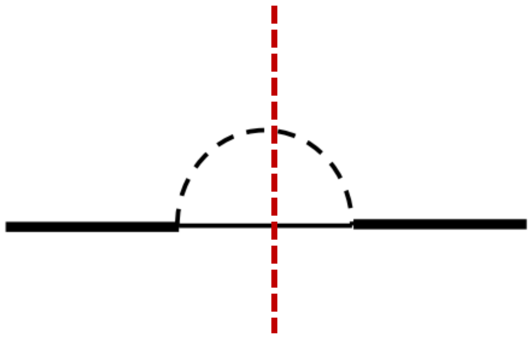

Table 6. The width (unit: keV) of the pole found in the DD^* and $D\bar{D}^*$ systems. The isospin conserved condition in the $D\bar{D}^*$ system is not included since the isospin breaking effect is large.

	isospin conserving	isospin breaking	isospin breaking and kinetic energies
DD^*	42	78	36
$D\bar{D}^*$	-	34	15

Phys. Rev. D 110 (2024) 5, 5

Measurement of the pole width of X(3872)

BESIII [64]	Pole	$(0.0068^{+0.1655}_{-0.1700}) - (0.190^{+0.206}_{-0.161})i$
LHCb [63]	Pole	$(0.06^{+0.16}_{-0.16}) - (0.13^{+0.32}_{-0.18})i$

Three mechanisms of producing the pole width of X(3872)

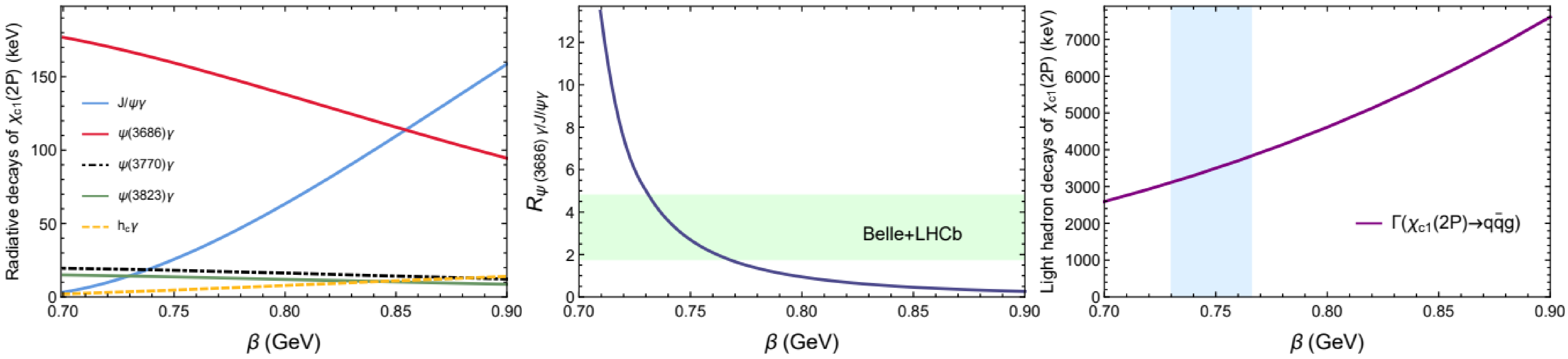

$$\mathcal{V}_{ij}(\mathbf{q},\mathbf{q}') = \frac{\mathcal{V}_{i0}(\mathbf{q}')\mathcal{V}_{0j}(\mathbf{q})}{E-M_0+i\epsilon} \to \frac{\mathcal{V}_{i0}(\mathbf{q}')\mathcal{V}_{0j}(\mathbf{q})e^{-\lambda^2(\mathbf{q}^2+\mathbf{q}'^2)}}{E-M_0+i\frac{1}{2}(\Gamma_a+\Gamma_b)}$$

$$\beta = 0.75 \text{ GeV}$$

$$\Gamma_a = 3488 \text{ keV and } \Gamma_b = 220 \text{ keV}$$

The magnitude of one MeV (compared with the ground state $\chi_{c1}(1P)$)

1. Three-body threshold cut
2. The self-energy of D^*
3. The transformation from the non-open charm decays of bare $\chi_{c1}(2P)$

The pole width of X(3872) in the full scattering amplitude

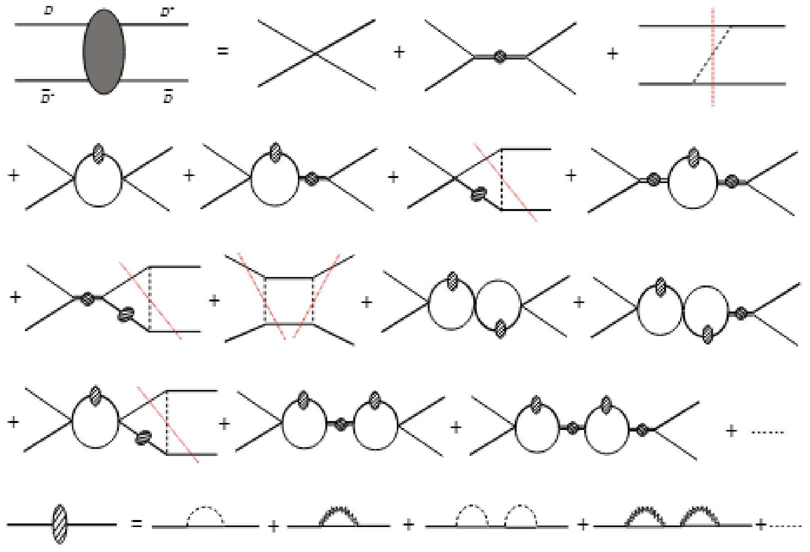

FIG. 3. The full Feynman diagram of the $D\bar{D}^* \to D\bar{D}^*$ scattering in the coupled-channel dynamics. The self-energy diagram from the non-open-charm decays for the bare χ'_{c1} is marked by shadow circle.

TABLE I. The poles and component possibilities of $X(3872)$ and a new resonance in the complete coupled-channel dynamics. The pole of $X(3872)$ is given by the binding energy relative to the $D^0\bar{D}^{*0}$ threshold. The χ and M superscripts denote the dressed χ'_{c1} resonance and the distorted $D\bar{D}^*$ resonance in the $(-,-)$ sheet, respectively. Here, $V_{ct}^{I=1} = 0$ GeV^{-2} and all pole positions are in units of MeV.

λ ($V_{ct}^{I=0}$) GeV^{-1} (GeV^{-2})			0.5 (96.6)	1.0 (22.5)	1.25 (11.2)	1.5 (3.7)	2.5 (-13.1)
Without $\Gamma_a + \Gamma_b$	$X(3872)$	Pole	-0.086-0.003i	-0.140-0.024i	-0.097-0.027i	-0.089-0.029i	-0.075-0.030i
With $\Gamma_a + \Gamma_b$	$X(3872)$	Pole	-0.059-1.36i	-0.060-0.293i	-0.060-0.164i	-0.070-0.119i	-0.071-0.065i
		$\mathcal{P}_{D^0\bar{D}^{*0}}$	0.145-0.015i	0.748-0.136i	0.858-0.078i	0.895-0.047i	0.939-0.013i
		$\mathcal{P}_{D^+\bar{D}^{*-}}$	0.110+0.002i	0.092+0.049i	0.065+0.035i	0.056+0.024i	0.043+0.009i
		$\mathcal{P}_{\chi'_{c1}}$	0.745+0.013i	0.160+0.087i	0.077+0.043i	0.049+0.023i	0.018+0.004i
	New resonance	Pole	4150-141i^M	4063-129i^M	4025-92i$^\chi$	4004-57i$^\chi$	3977-8i$^\chi$
		$\mathcal{P}_{D^0\bar{D}^{*0}}$	0.328+0.048i	0.278-0.191i	0.203-0.255i	0.104-0.209i	0.088-0.040i
		$\mathcal{P}_{D^+\bar{D}^{*-}}$	0.324+0.007i	0.265-0.219i	0.187-0.286i	0.086-0.234i	0.092-0.062i
		$\mathcal{P}_{\chi'_{c1}}$	0.348-0.055i	0.457+0.410i	0.610+0.541i	0.810+0.443i	0.820+0.102i
BESIII [64]		Pole	$(0.0068^{+0.1655}_{-0.1700}) - (0.190^{+0.206}_{-0.161})i$				
LHCb [63]		Pole	$(0.06^{+0.16}_{-0.16}) - (0.13^{+0.32}_{-0.18})i$				

A novel approach to reveal the nature of X(3872)

LHCb: Observation of a new 1^{++} charmoniumlike state $\chi_{c1}(4010)$

Phys. Rev. Lett. 133, 131902 (2024)

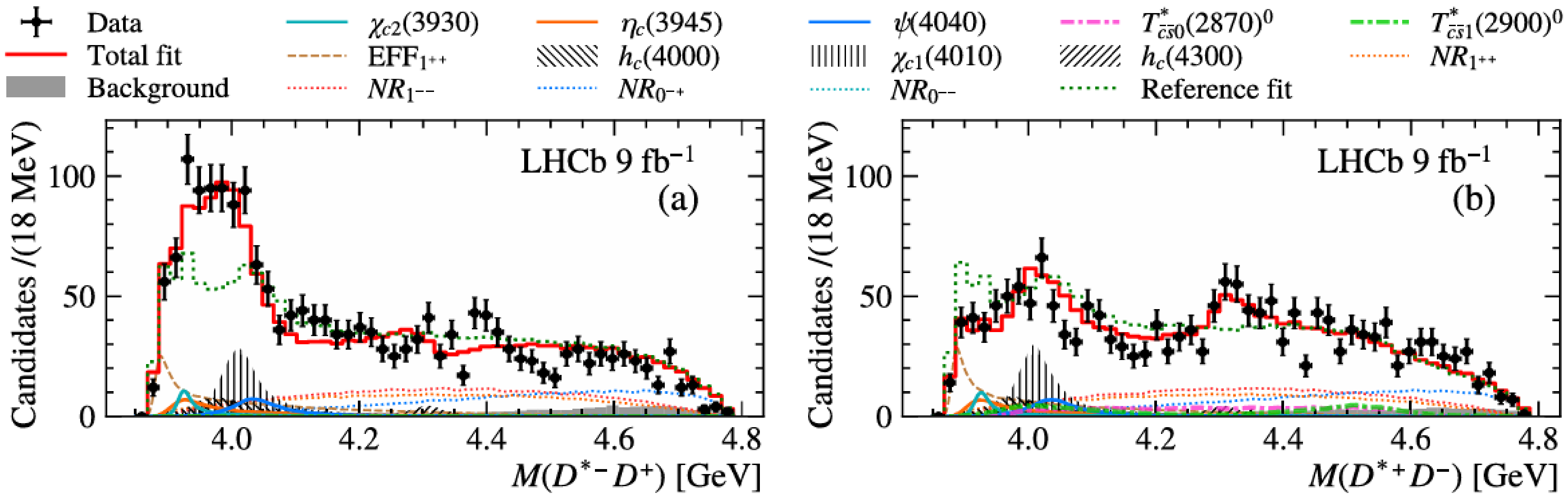

Our work: arXiv:2404.16575

$\chi_{c1}(4010)$ $\quad J^{PC} = 1^{++}$

$m_0 = 4012.5^{+3.6}_{-3.9}{}^{+4.1}_{-3.7}$ $\quad \Gamma_0 = 62.7^{+7.0}_{-6.4}{}^{+6.4}_{-6.6}$

LHCb: arXiv:2406.03156

	Pole	4150-141i^M	4063-129i^M	4025-92i^X	4004-57i^X	3977-8i^X
New resonance	$\mathcal{P}_{D^0\bar{D}^{*0}}$	0.328+0.048i	0.278-0.191i	0.203-0.255i	0.104-0.209i	0.088-0.040i
	$\mathcal{P}_{D^+\bar{D}^{*-}}$	0.324+0.007i	0.265-0.219i	0.187-0.286i	0.086-0.234i	0.092-0.062i
	$\mathcal{P}_{\chi'_{c1}}$	0.348-0.055i	0.457+0.410i	0.610+0.541i	0.810+0.443i	0.820+0.102i

The LHCb observation is consistent with our prediction

A novel approach to reveal the nature of X(3872)

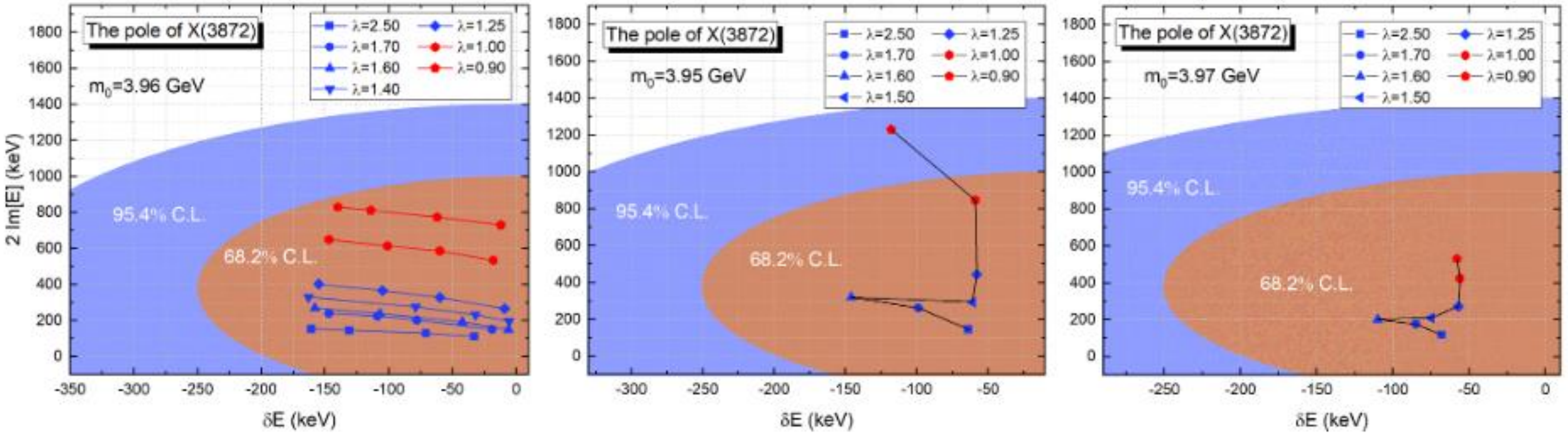

FIG. 5. The experimental constraints on the pole position of $X(3872)$. The shaded region represents the confidence level for the pole distribution possibility of $X(3872)$ based on the experimental data. The solid dots represent the theoretical pole positions of $X(3872)$, with red and blue representing the solutions in the strong and weak coupling modes, respectively. The subfigures, from left to right, correspond to the bare mass values $m_0 = 3.96, 3.95, 3.97$ GeV for the χ'_{c1}. Here, the dots with the same pattern refer to theoretical results with the same λ but different coupling constant $V_{ct}^{I=0}$, whose impact is almost reflected in the binding energy of $X(3872)$ and is therefore only shown in the subfigure on the left.

A novel approach to reveal the nature of X(3872)

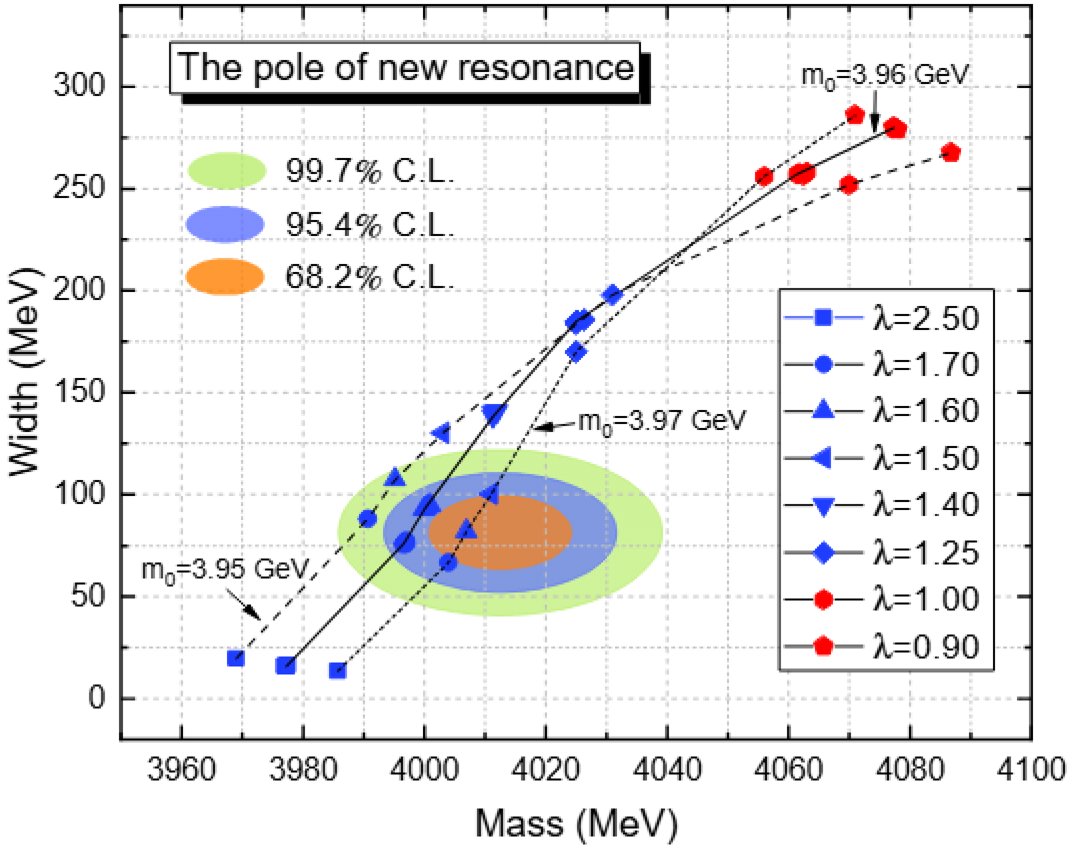

FIG. 6. The experimental constraints on the pole position of the predicted new resonance. The shaded region represents the confidence level for the pole distribution possibility of $\chi_{c1}(4010)$ based on the LHCb data. The solid dots represent the theoretical pole positions of the new resonance, with red and blue representing the solutions in the strong and weak coupling modes, respectively.

The confirmation and precise measurement of higher new resonance can indeed provide very effective way for uncovering the mystery of X(3872)

Summary

- In the coupled channel dynamics, we demonstrate that the X(3872) does not stem from the mass shift of bare χ_{c1}' state.

- We reveal that the X(3872) stems from either the $D\bar{D}^*$ pole or the shadow pole of χ_{c1}'.

- If the $\boldsymbol{\chi_{c1}(4010)}$ can be confirmed by other experiment, by matching it to our predicted resonance, we conclude that the X(3872) most likely originates from the $\mathbf{D\bar{D}}^*$ pole with a confidence level exceeding 99.7%.

Thanks for your attention!